Effect of lattice strain on X-ray Diffraction, Raman Spectroscopy and Optical Properties of as Synthesis Nanocomposite ZnO-SnO_2-TiO_2 Thin Film by Spray Pyrolysis Method

Sudhir Kumar and B. Das

Advanced Material Research Lab, Department of Physics,
University of Lucknow, Lucknow,India- 226007.
Email:skvma88@gmail.com, bdas226010@gmail.com

ABSTRACT

The nanocomposite ZnO-SnO_2-TiO_2 thin films were synthesized via spray pyrolysis method. They were studied by X-ray diffraction (XRD) and Raman spectroscopy in order to determinate a film composition and structural properties. The effect of annealing temperatures on the crystalline structure and optical property was investigated. The surface morphologies of the thin films were studied by using atomic force microscopy (AFM). At low annealing temperature (700 ^{0}C) thin film shows amorphous in nature. The crystallinity of thin film was achieved at annealing temperature $\geq$ 750 ^{0}C. The broadening of XRD and Raman peaks are mainly due to the lattice strain present in the nanocomposite thin films which results the decreased in intensity of the peaks. An AFM image shows that the grains are nearly in spherical shape and they increases with annealing temperature. The optical band gaps of thin films were calculated by using UV. Vis. Spectroscopy and found 3.68 eV, 3.70 eV, 3.74 eV and 3.76 eV at annealing temperature 700 ^{0}C, 750 ^{0}C, 850 ^{0}C and 900 ^{0}C respectively.

Keywords:-Nanocomposite ZnO-SnO_2-TiO_2 Thin Film, XRD, W-H Plot, Raman, AFM, Lattice Strain.

1. Introduction

Thin films of nanocomposite considered at least two phases, an amorphous phase and nanocrstalline phase, or a nanocrstalline phase with another nanocrstalline phase. Due to the unique physical-chemical properties [1-2], structural [3] and optical [4] the nanocomposite films have received much attention recently. To synthesis of nanocomposite thin films many factors are necessary for considerations during synthesis such as surface and interfacial energy, the interface volume, crystallite size, epitaxial stress and strain, texture etc. The metal oxides such as ZnO, SnO_2, TiO_2, CuO, WO_3 etc. are very important for technologically as well as fundamental point of view. The Synthesis and fabrication of nanocomposite thin films based on semiconducting oxides is an important goal for the obtainment of improved functional performances in advanced fields such as sensing, optoelectronics, and catalysis. Recently, the fabrication of materials showing novel technological applications mixed metal oxides or binary semiconducting systems have attracted more and more attention have been prepared and some researchers pointed out that they were promising candidates for electronic instruments. To enhance the mechanical and photocatalytic property of TiO_2 many researchers have been prepared composites with TiO_2 for example ZnO-TiO_2 [5], SnO_2-TiO_2 [6] etc. The coupled oxide semiconductor shows efficient charge separation which suppress the charge recombination in nanoporous dye sensitized photoelectrochemical (DSPE) solar cells, nanocrystalline coupled semiconductor electrodes of the type OTE/SnO_2/TiO_2 have been prepared[7]. The composite SnO_2/TiO_2/SnO_2 system has a higher surface energy than the individual SnO_2 and TiO_2 oxides whereas for the TiO_2/SnO_2/TiO_2 the corresponding values are of the same order that of TiO_2 oxide and lower than those of SnO_2 oxide has been calculated theoretically by using density functional theory [8].

To the best of our knowledge, there are no reports on the synthesis of composite ZnO-SnO_2-TiO_2 thin film. In this study, ZnO-SnO_2-TiO_2 nanocomposite thin films were synthesized by a Spray pyrolysis method and were characterized using X-ray diffractometer (XRD), micro Raman spectrometer, UV-Vis.-NIR spectroscopy and atomic force microscope (AFM).

2. Experimental details

The number of thin film nanocomposite of ZnO, SnO_2, and TiO_2 of energy band gaps of 3.4 eV, 3.6 eV and 3.2 eV respectively were synthesized by spray pyrolysis method. Zinc acetate dihydrate $Zn(CH_3COO)_2.2H_2O$ (Merck, India), tinchloride dihydrate $SnCl_2.2H_2O$ (Merck, India) and titanium tetra chloride $TiCl_4$ (Merck, India) were used as precursor and ethanol (C_2H_5OH) and hydrochloric acid (HCl) were used as solvent.

4.3898gm of $Zn(CH_3COO)_2.2H_2O$ (1M) was dissolved in mixture of 16ml ethanol+4ml HCl, and stirred at room temperature for 6 h. The transparent solution of $[Zn(CH_3COO)_2+C_2H_5OH+HCl]$ was obtained;4.5126gm of $SnCl_2.2H_2O$ (1M) was dissolved in mixture of 16ml ethanol+4ml HCl, and stirred at room temperature for 6 h. The transparent solution of $[SnCl_2+C_2H_5OH+ HCl]$ was obtained; 2.2ml of $TiCl_4$(1M) was dissolved in mixture of 16ml ethanol+4ml HCl, and stirred at 80 ^{0}C temperature for 6 h. The transparent solution of $[TiCl_4+ C_2H_5OH +HCl]$ was obtained.

Now solutions $[Zn(CH_3COO)_2+ C_2H_5OH+ HCl]$,$[SnCl_2+C_2H_5OH+ HCl]$ and$[TiCl_4+ C_2H_5OH +HCl]$ were mixed together, and stirred at room temperature for 10 h to get the homogenous transparent solution. The homogenous solution were sprayed on glass substrates at 400 ^{0}C. The deposited films were annealed at 700 ^{0}C, 750 ^{0}C, 800 ^{0}C, 850 ^{0}C and 900 ^{0}C for 30 minutes for crystallinity. Film deposition process by spray pyrolysis method was summarised as in fig. 1: The X-ray diffraction pattern was recorded by using powder X-ray diffractometer (Bruker D8 Advance) at room temperature with monochromatic CuK_α radiation (λ=1.5406 Å) in a wide range of Bragg angle 2θ from 20º to 70º with scanning rate of 0.5º min^{-1}. The Raman spectra were recorded by using Micro Raman spectrometer (JobinYvonHoribra LABRAM-HR) at room temperature in the range of wave-number from 100 cm^{-1} to 1300 cm^{-1}. The surface morphology and roughness of nanocomposite thin films were carried out with the help of Atomic Force Microscope (AFM) (SPM Digital Instrument NanoscopeIIIa), the absorptions spectra were recorded by using UV-Vis.-NIR spectrophotometer (Perkin Elmer, USA. Model:Lambda 950) in the wavelength range 200-858nm.

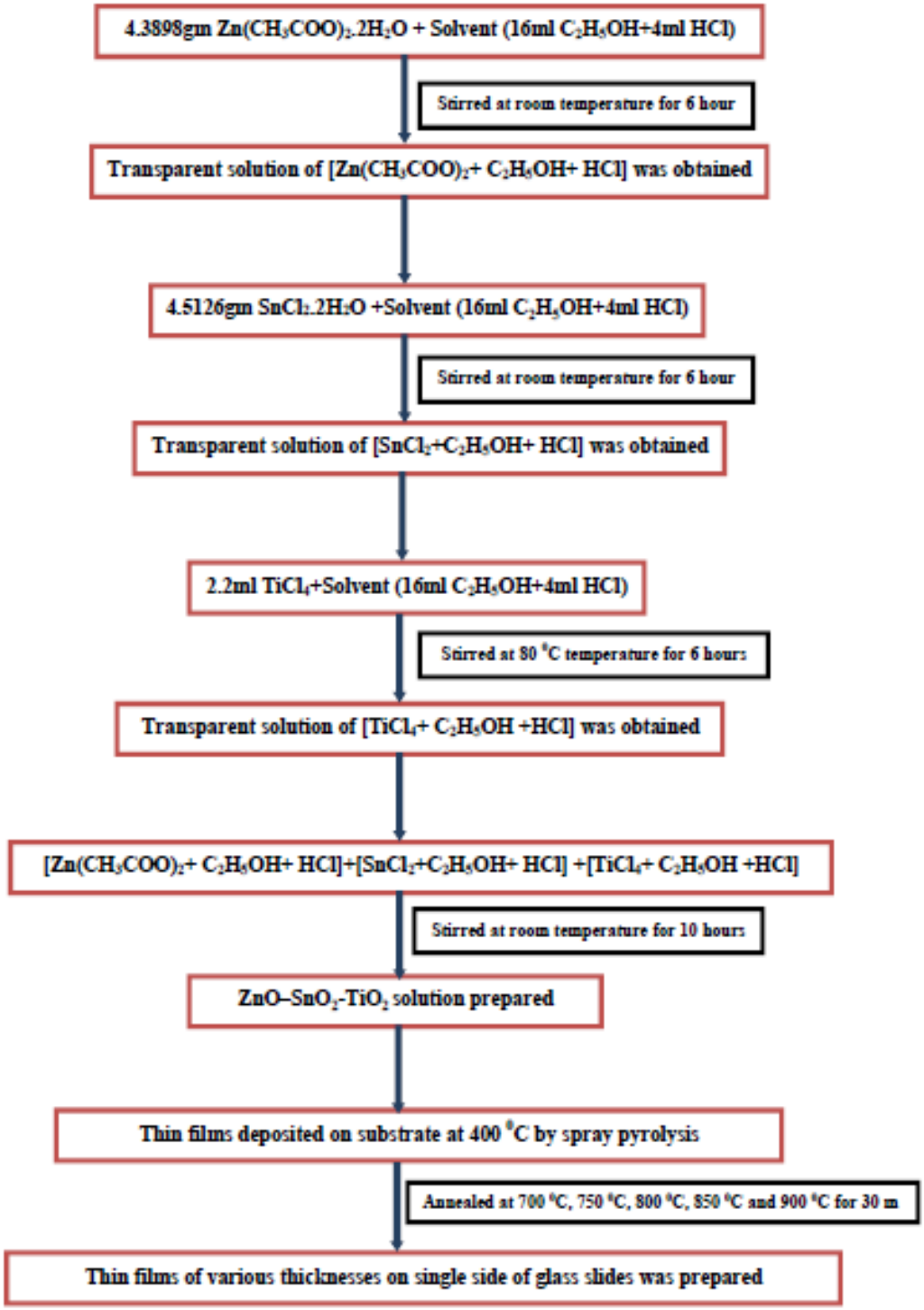

Figure 1: Flow chart of synthesis of nanocomposite ZnO-SnO_2-TiO_2 thin film by spray pyrolysis method .

3. Results and Discussion

3.1 X-Ray Diffraction Analysis

XRD was employed to determine the phase analysis of each thin film annealed at increasing temperatures as shown in fig. 2. It can be seen that the film is amorphous annealed at 700 ^{0}C. When the temperature increased to 750 ^{0}C, as shown in fig. 2 seven diffraction peaks are found, which belong to (110), (221), (220) tetragonal rutile phase of TiO_2 with space group $P4_2/mnm$ (JCPDS No. 21-1276), (221) orthorhombic brookite phase of TiO_2 with space group Pcab (JCPDS No. 29-1360), (101) tetragonal rutile phase of SnO with space group P4/nmm (JCPDS No. 06-0395), (310) tetragonal rutile phase of SnO_2 with space group $P4_2/mnm$ (JCPDS No. 01-077-0449) and (002) hexagonal wurtzite phase of ZnO with space group $P6_3mc$ (JCPDS No. 89-1397). Further, as annealing temperature was increased (221) diffraction peak disappeared at 800 ^{0}C, 850 ^{0}C and 900 ^{0}C respectively. At annealing temperature 900 ^{0}C the intensity of the (310) diffraction peak was almost zero. The above XRD results show that the structure of the thin films changed from amorphous to crystalline phase with the increasing of the annealing temperature. The Crystallite size and the lattice strain were determined for each crystalline thin film by adopting the Williamson-Hall (W-H) equation [9].

$$\beta Cos\theta = \frac{0.9\lambda}{D} + 4\varepsilon Sin\theta \qquad (1)$$

In equation 1, λ is the wavelength of X-ray radiation, β is the full width at half maximum (FWHM) and θ is the diffraction angle of the diffraction peaks. D is the effective crystallite size with lattice strain, and ε is the effective value of lattice strain. βCosθ is plotted against 4Sinθ, and after linear fitting, the intercept gives the value of D and the slope gives the value of ε. Fig. 3(a), 3(b), 3(c) and 3(d) illustrates the W-H plot of all the crystalline nanocomposite ZnO-SnO_2-TiO_2 thin films. The value of crystallite size and of lattice strain of each crystalline thin film is inserted in Table 1. As evident from Table 1, film annealed at 800 ^{0}C exhibits the highest lattice strain, whereas film annealed at 900 ^{0}C has the lowest. Positive strain shows the system is under tensile strain while negative strain compressive strain. As the temperature increases the crystallite size also increases due to the increase in thermal energy which confirms from Table 1. There is a nonuniform strain developed in the thin film because their strain value does not show regular

variation with the annealing temperature. Due to nonuniform strain the shape of the peak will change and peak will become broaden and the resultant intensity will decrease. This is the

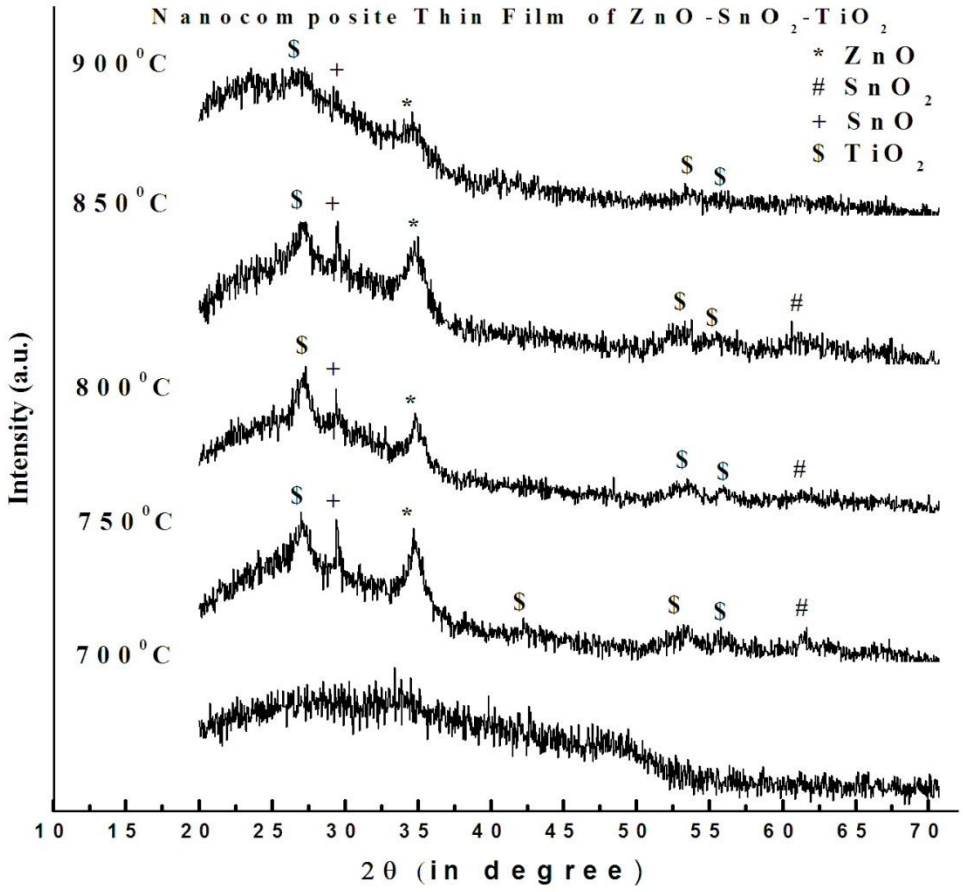

Figure 2: XRD of the nanocomposite ZnO-SnO_2-TiO_2annealed at 700 ^{0}C, 750 ^{0}C, 800 ^{0}C, 850 ^{0}C and 900 ^{0}C temperature.

main reason that (221) and (310) diffraction peaks intensity becomes zero and finally disappeared at annealing temperature 900 ^{0}C also the intensity decreases of the diffraction peaks (110), (101), (221) and (220) with the annealing temperature as show in fig. 2.The mechanism of broadening of the X-ray diffraction peak due to strain is illustrated in fig. 4. If there is no strain in a portion of the grain, the spacing between the planes everywhere is same and equilibrium spacing is d. The diffraction on line from these planes appearson the right as shown in fig. 4(a). If the uniform tensile strain is applied at right angles to the reflecting planes, their spacing becomes larger than d, and the corresponding diffraction line shifts to lower angles without any

change in shape and size as shown in fig. 4(b). However the behavior of the diffraction peak is totally different when the nonuniform strain is applied to the reflecting planes. The grain is bent in presence of nonuniform strain, on the top (tension) side the plane spacing exceeds d, on the

Table 1Crystallite size, lattice strain, particle size and roughness of the nanocomposite ZnO- SnO_2- TiO_2 thin films

Annealing Temperature (^{0}C)	**Crystallite Size (nm)**	**Lattice Strain (ε)**	**Particle Size (nm)**	**Roughness (nm)**
700	-	-	68	1.67
750	11	0.00341	74	1.22
800	27	0.01738	-	-
850	30	0.01702	109	1.78
900	34	-0.01631	-	9.81

bottom (compression) it is less than d, and somewhere in between it equals d. We may imagine this grain to be composed of a number of small regions in each of which the plane spacing is substantially constant but different from the spacing in adjoining regions. These regions cause the various sharp diffraction lines indicated on fig. 4(c) within the broad peak. The sum of these sharp lines, each slightly displaced from the other, is the broadened diffraction line shown by curve in fig. 4(c) [10].

3.2. Raman Spectroscopy Analysis

Raman spectroscopy was employed to phase identification of the as synthesized nanocomposite ZnO-SnO_2-TiO_2 thin film by spray pyrolysis method. The Raman spectra of the annealed nanocomposite thin films at increasing temperature along with their modes of the nanocomposite are shown in fig. 5. At annealing temperature 700 ^{0}C and 800 ^{0}C two Raman peaks at wavenumber 564 cm^{-1} and 1098 cm^{-1} are observed which belong to vibrational mode A_1(LO) and 2LO of hexagonalwurtzite ZnO [11] phase also one Raman peak at wavenumber 660 cm^{-1} assigned vibrational mode E_g of tetragonal anatase phase [12] at 800 ^{0}C.The above result indicates that at annealing temperature 700 ^{0}C the formation of nanocomposite was not

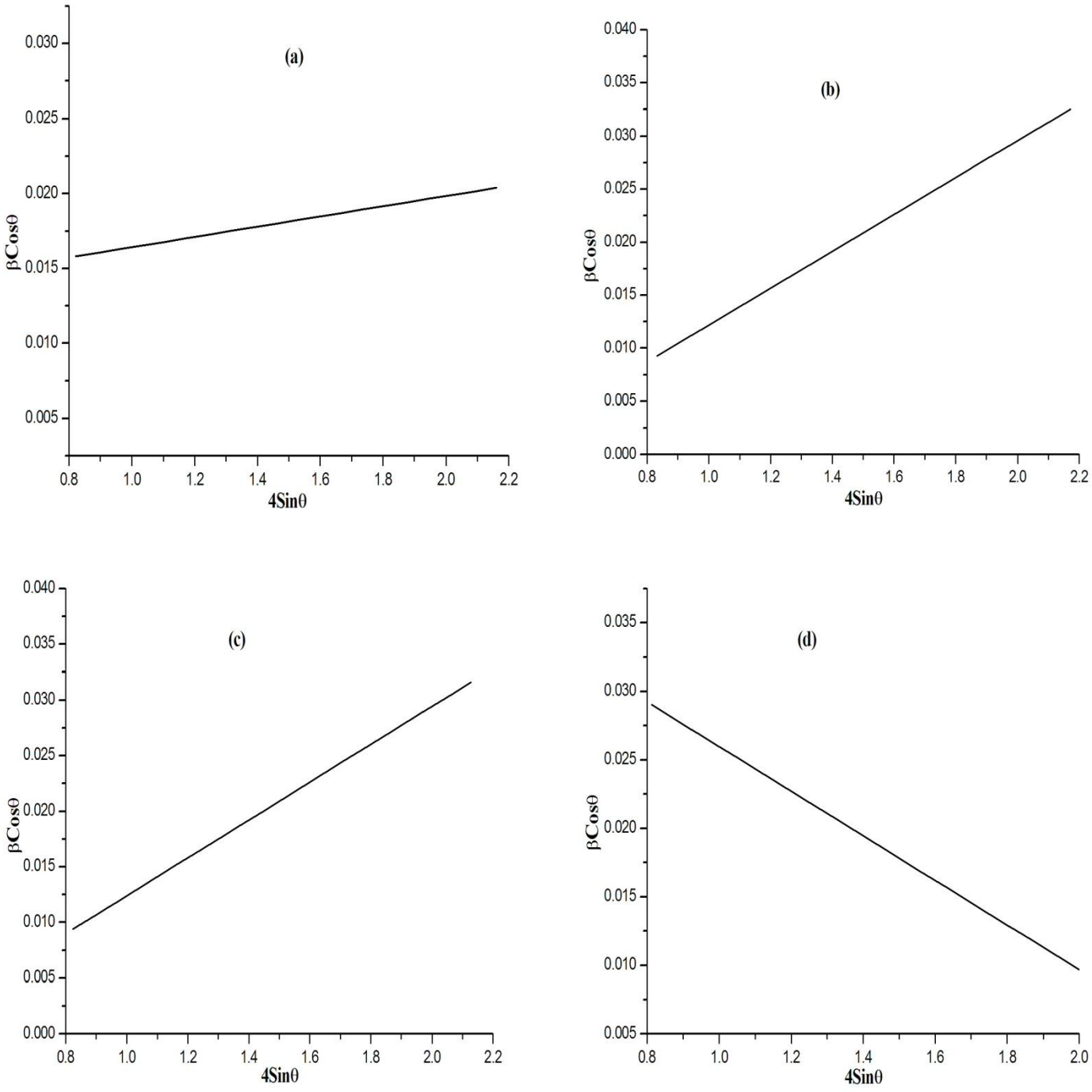

Figure 3: W-H plot of nanocomposite ZnO-SnO_2-TiO_2 thin film annealed at (a) 750 ^{0}C, (b) 800 ^{0}C, (c) 850 ^{0}C and (d) 900 ^{0}C.

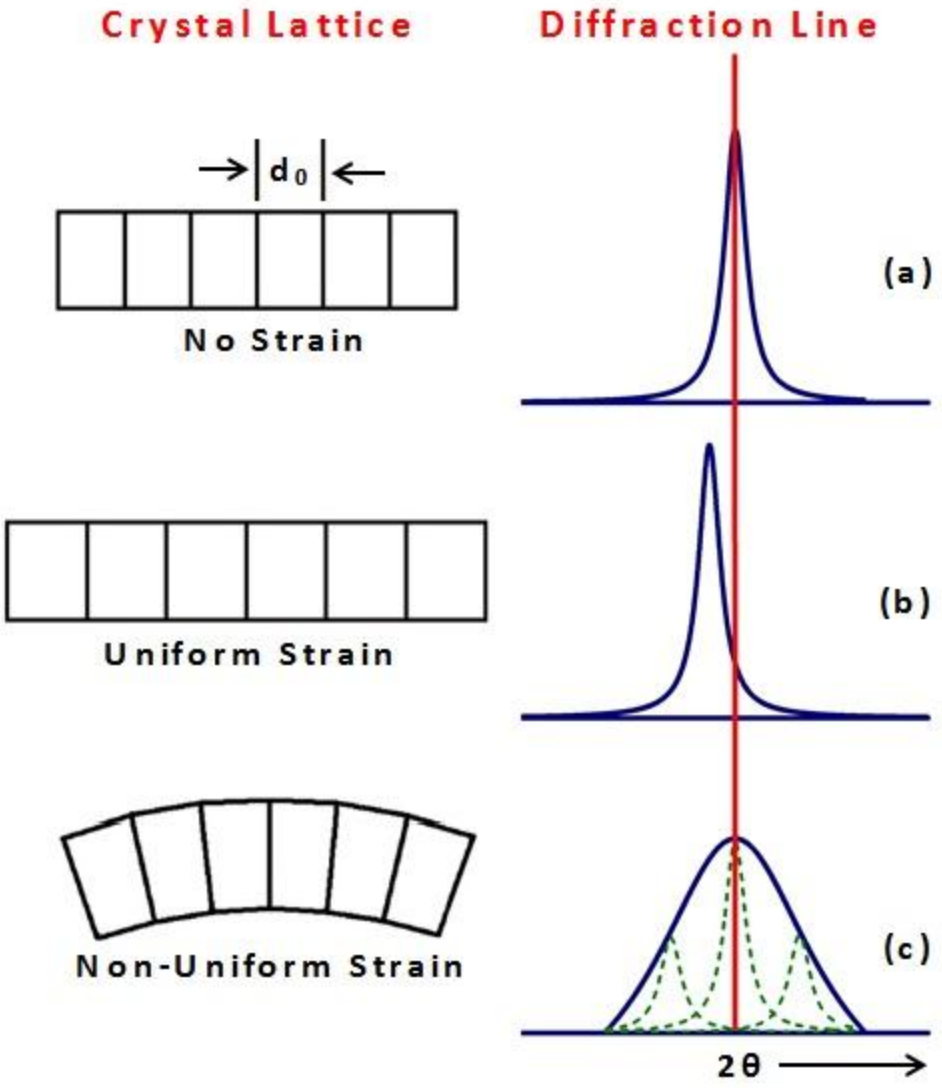

Figure 4: Effect of Lattice strain on X-ray Diffraction Line

At annealing temperature 750 ^{0}C eleven Raman peaks are observed, in which out of two Raman peak at wavenumber 117 cm^{-1} and 151 cm^{-1} belong to the vibrational mode E_g and A_{1g} of a brookite TiO_2 phase [13-14], two Raman peak at wavenumber 235 cm^{-1} and 316 cm^{-1} belong to vibrational mode B_{1g} and one at wavenumber 615 cm^{-1} belong to vibrational mode A_{1g} of rutile TiO_2 phase[13], two Raman peak of vibrational mode B_{2g} at wavenumbers 276 cm^{-1} and 784 cm^{-1} and one Raman peak at wavenumber 713 cm^{-1} of vibrational mode E_u(LO) belong to tetragonal SnO_2 phase [15] and remaining three Raman peaks at wavenumber 435 cm^{-1}, 671 cm^{-1} and 1095 cm^{-1} belong to vibrational mode E_2^{high}, TA+LO and 2LO hexagonal wurtzite ZnO

phase [11, 16]. As from above results, clears the formation of nanocomposite ZnO-SnO_2-TiO_2 thin film as revealed by the presence of ZnO, SnO_2 and TiO_2 phase.

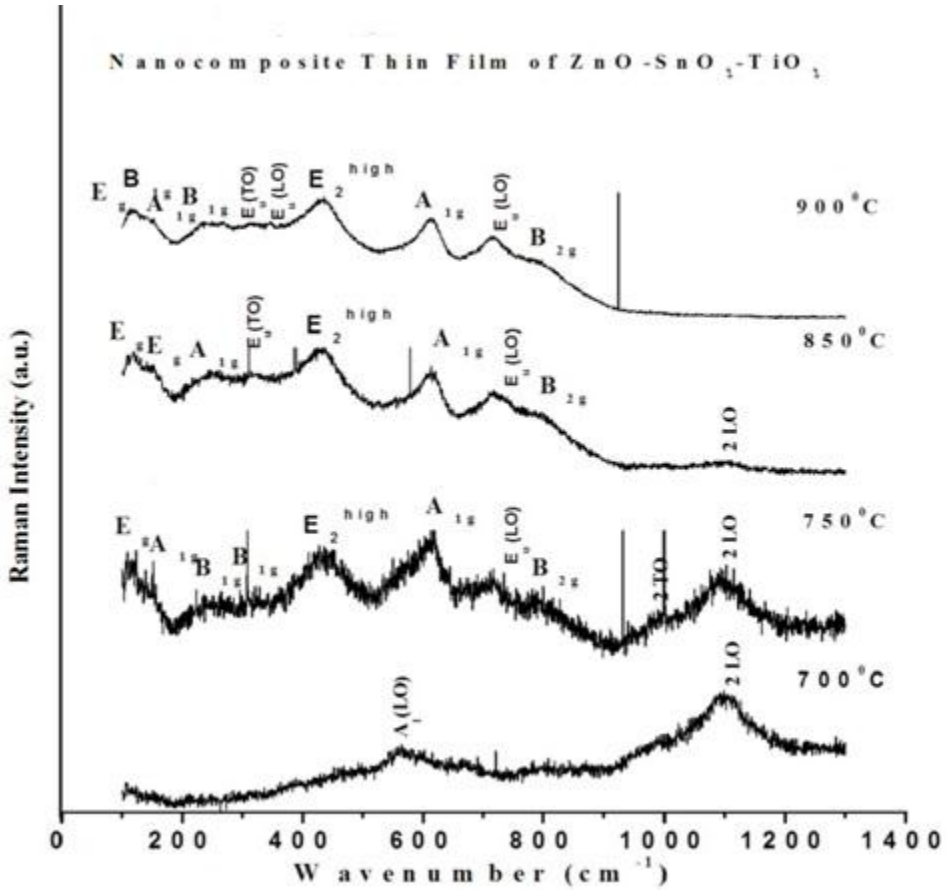

Figure 5: Raman spectra of nanocomposite ZnO-SnO_2-TiO_2thin film annealed at 700 ^{0}C, 750 ^{0}C, 850 ^{0}C and 900 ^{0}C temperature.

As the annealing temperature increased to 850 ^{0}C, three new Raman peaks are observed at wavenumber 146 cm^{-1}, 256 cm^{-1} and 306 cm^{-1} which belong to vibrational mode E_g anatase TiO_2 phase, A_{1g} rutile TiO_2 and E_u(TO) tetragonal SnO_2 phase. The Raman vibrational mode E_g, E_2^{high}, A_{1g}, E_u(LO), B_{2g} and 2LO occurs at wavenumber 119 cm^{-1}, 431 cm^{-1}, 613 cm^{-1}, 716 cm^{-1}, 791 cm^{-1} and 1102 cm^{-1} respectively at this annealing temperature. At annealing temperature 900 ^{0}C two new Raman peaks at wave number 121 cm^{-1} and 347 cm^{-1} belong to vibrational mode B_{1g} and E_u(LO) tetragonal SnO_2 phase [15, 17] are occur which are not present at annealing temperature 750 ^{0}C and 850 ^{0}C. Also at this temperature Raman shifts of vibrational mode E_u(TO), A_{1g}, E_u(LO) and B_{2g} takes place and Raman peaks are found at wavenumber 310 cm^{-1},

612 cm^{-1}, 714 cm^{-1} and 792 cm^{-1} respectively while in vibrational mode A_{1g} brookite TiO_2 phase and B_{1g} rutile TiO_2 phase there is found no shifting.

However, it is noticed that along with the increasing of the annealing temperature the intensity of the Raman vibrational modes reduced gradually, also the peaks are broadened as shown in fig. 5. The decreased in intensity and broadening of Raman peaks are mainly due to the presence of lattice strain and crystallite size in the grains of a nanocomposite ZnO-SnO_2-TiO_2 thin films.

3.3 UV. Vis. NIR Spectroscopy

Optical characterization of nanocomposite thin films gives more information such as optical band gap, band structure, optically active defects etc. The band gap of the nanocomposite ZnO-SnO_2-TiO_2 thin film was determined by fitting the absorption data to the direct transition:

$$\boldsymbol{\alpha h\nu = A(h\nu - Eg)^{1/2}} \quad \ldots (\mathbf{2})$$

Where $\boldsymbol{\alpha}$ is the linear optical absorption coefficient, hν is the photon energy, Eg is the direct band gap and A is a constant [18]. The band gap of nanocomposite ZnO-SnO_2-TiO_2 thin film was measured by plotting $(\boldsymbol{\alpha}h\nu)^2$ as a function of photon energy hν, and extrapolation the linear portion of the curve to absorption equal to zero as given in fig. 6. The band gap of the nanocomposite at annealing temperature 700 ^{0}C, 750 ^{0}C, 850 ^{0}C and 900 ^{0}C are 3.68 eV, 3.70 eV,3.74 eV and 3.76 eV respectively. The band gap slightly increases with the annealing temperature as shown in fig. 6. The inter-atomic spacing of semiconductors changes due to the strain which affects the energy band [19] and band gap increases for increase in compressive strain while decreases for increase in tensile strain [20-21]. However there are only a little bit changes in the energy band gap as strain changes of the thin film. The lowest tensile strain 0.00341 occurs at annealing temperature 750 ^{0}C which corresponds to band gap 3.70 eV while compressive strain -0.01631occurs at annealing temperature 900 ^{0}C which corresponds to band gap 3.76 eV.

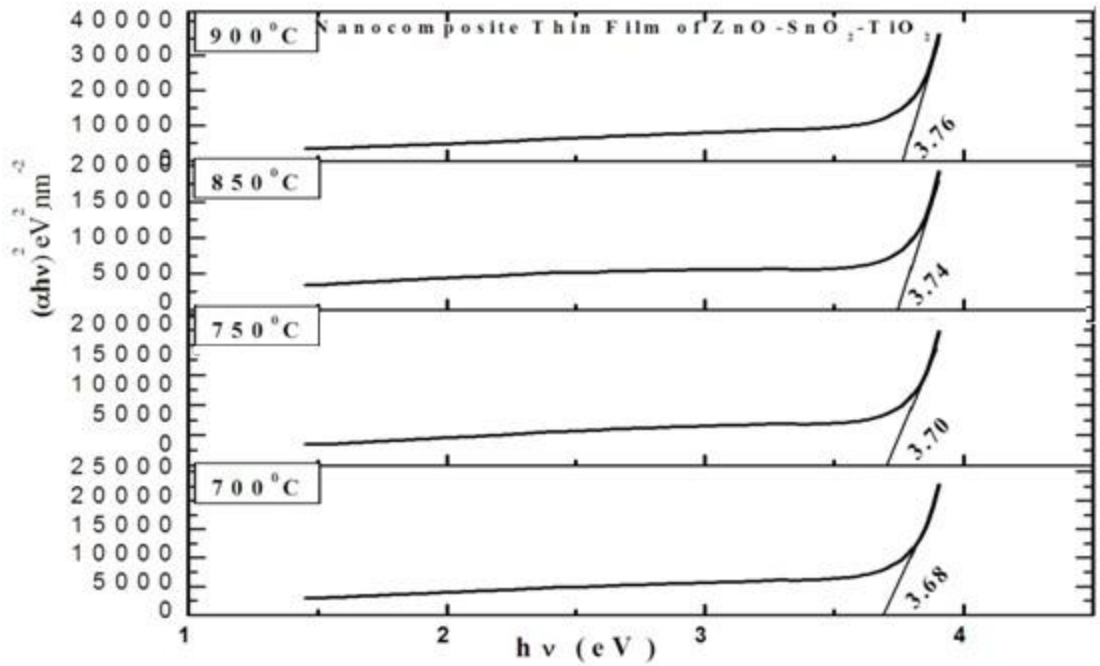

Figure 6: Plot $(\alpha h\nu)^2$ vs hν of nanocomposite ZnO-SnO_2-TiO_2 thin film annealed at 700 ^{0}C, 750 ^{0}C, 850 ^{0}C and 900 ^{0}C.

3.4 Atomic Force Microscopy

Since the atomic force microscopic technique is powerful methods for providing the information about the surface morphology (e.g. porosity, cracks, roughness, size, and orientation of grains etc.) of as synthesized nanocomposite thin films at different annealing temperatures. The studies of thin film surface morphologies were carried out by using atomic force microscopy measurement. All thin films were scanned at several different locations on the film surface. Surface morphologies vary significantly among nanocomposite ZnO-SnO_2-TiO_2 thin films annealed at different temperatures. Fig. 7 shows AFM image from those films annealed at different temperatures but at the same initial conditions. They show the effect of annealing temperature on thin film morphology. As the annealing temperature increases particle size also increases. This increase in size of particle is due to the agglomeration of the crystallites. As the temperature increases more and more crystallite agglomeration takes place which result the increased of the size of the particle as shown in fig. 7. The shape of the particle size is nearly

spherical as revealed from the AFM images. The variation of particle size and roughness with annealing temperature are shown in table 1.

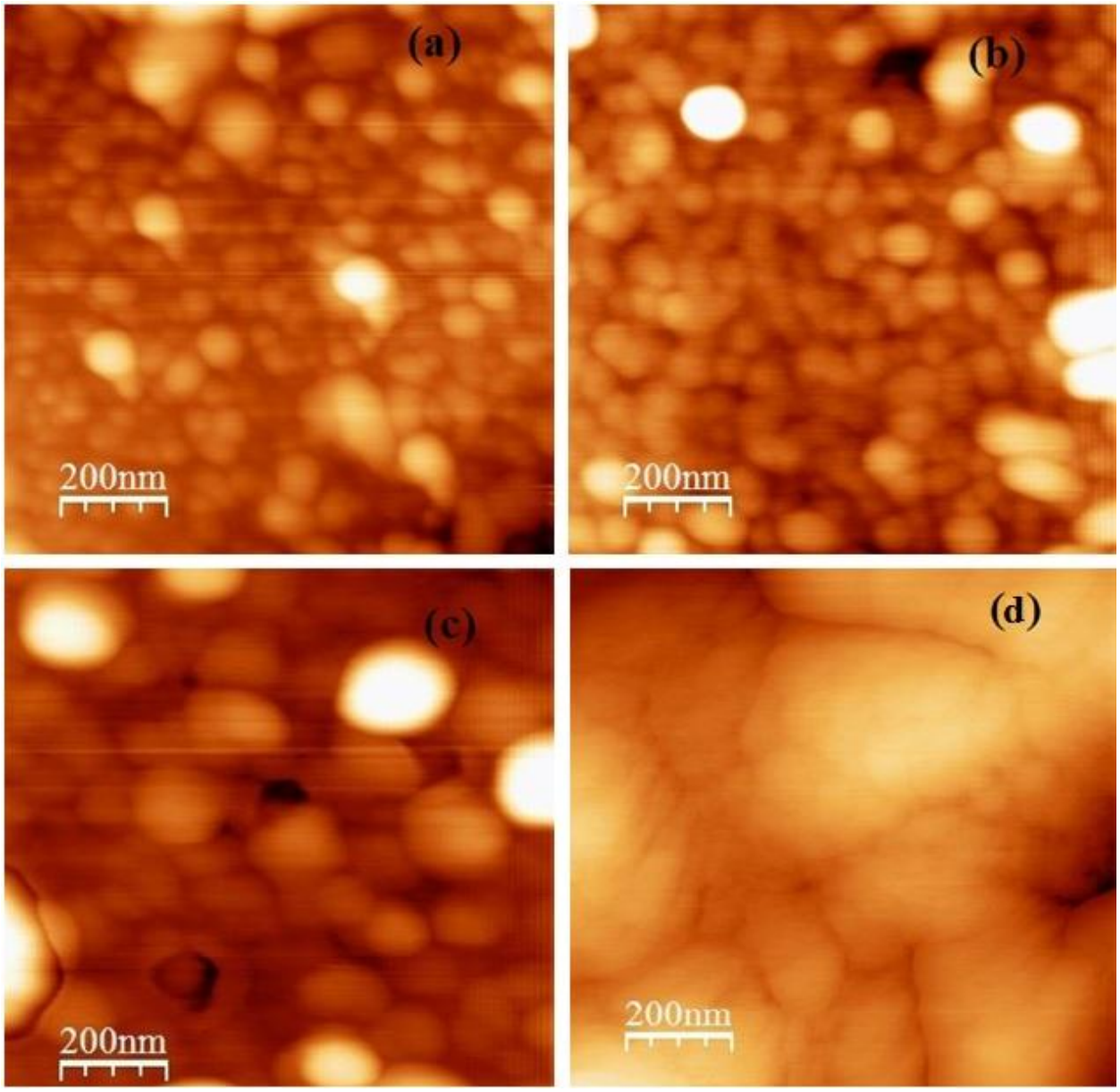

Figure 7: AFM image of nanocomposite ZnO-SnO_2-TiO_2 annealed at (a) 700 ^{0}C, (b) 750 ^{0}C, (c) 850 ^{0}C and (d) 900 ^{0}C.

4 Conclusions

Nanocomposite ZnO-SnO_2-TiO_2 thin films were prepared by spray pyrolysis method. At annealing temperature 700 ^{0}C the XRD result shows the amorphous in nature of thin film deposited on glass substrate. The crystallinity of the thin films was achieved at higher annealing temperature. The XRD spectra of thin films show the broadening of the peak which results the decrease in intensity of the XRD reflection and at high annealing temperature (900 ^{0}C) some reflection are absent which were found at low annealing temperature (750 ^{0}C). The broadening is due to the presence of non-uniform lattice strain in the nanocomposite thin films. A Raman spectrum also shows the variation of intensity of vibrational mode dependence with lattice strain and crystallite size. An XRD and Raman spectrum both confirms the formation of nanocomposite thin film. The effect of strain on the band gap of thin films are also observed but in little bit amount. The band gap decreases as tensile lattice strain increases while increases as compressive lattice strain increases. AFM image shows that as annealing temperature increases particle size also increases due to the agglomeration of the crystallite. The grains of the nanocomposite thin films are nearly spherical in shape.

Acknowledgement:- The experiment was supported by UGC-DAE Consortium for Scientific Research Centre, Indore, India.

References:

[1] SherifEl-S M, Alam M A, Al-Zahrani S M. Fabrication of Different Protective Coatings and Studying Their Mechanical Properties and Corrosion Behavior in Sodium Chloridesolutions. Int. J. Electrochem. Sci.2015; 10:373-387.

[2] Musila J, Hruby H, Zeman P, Zeman H, Cerstvy R. Mayrhofer P H, Mitterer C. Superhardnanocomposite Al-Cu-N Films Prepareby Magnetron Sputtering. Surface and Coatings Technology 2001; 142-144:603-609.

[3] Pierson J F, Belmonte T, Michel H. Structural Characterization of ZrB_2/oxides Nanocomposite films Synthesized in flowing Ar-BCl_3 Post-Discharges. Applied Surface Science 2001; 172:285-294.

[4]Patil L A, Pathan I G, Suryawanshi D N, Patil D M. Effect on Structural, Micro Structural and Optical Properties Due to Change in Composition of Zn and Sn in ZnO:SnO_2Nanocomposite Thin Films. J. Nano- Electron. Phys. 2013; 5:02028-0234.

[5] Li D, Jiang X, Zhang Y, Zhang B. A Novel Route to ZnO/TiO_2Heterojunction Composite Fibers. J. Mater Res. 2013; 28:507-512.

[6]Yang J, Li D, Wang X, Yang X J, Lu L D. Rapid Synthesis of NanocrystallineTiO_2/SnO_2 Binary Oxides and their Photo Induced Decomposition of Methyl Orange. J. Solid State Chem.2002; 165:193-198.

[7]Nasr C, Kamat P V, Hotchandani S. Photosensitization of the SnO_2/TiO_2 Coupled System with a Rutheniumpolypyridyl Complex.J. Phys. Chem. B 1998; 102:10047-10056.

[8]Beltran A, Andres J, Sambrano J R, Longo E. Density Functional Theory Study on The Structural and Electronic Properties of Low Index Rutile Surfaces for TiO_2/SnO_2/$TiO_2$and SnO_2/TiO_2/SnO_2 Composite Systems.J. Phys. Chem. A 2008; 112:8943-8952.

[9] Williamson G K, Hall W H. X-ray Line Broadening from Field Aluminium and Wolfram.ActaMetall 1953; 1:22-32.

[10] Cullity B D. Element of X-ray Diffraction. Boston, Addison-Wesley Publishing Co,1956.

[11] Calleja J M, Cardona M. Resonant Raman Scattering in ZnO. Phys. Rev. B 1977; 16:3753-3761.

[12] Mikami M, Nakamura S, Kitao O, Arakawa H. Lattice Dynamics and Dielectric of TiO_2 Anatase: A First Principles Study.J. Phys. R. B 2002; 66:155213-1-6.

[13] Kremenovic A, Brojcin M G, Welsch A M, Colomban P. Heterogeneity in Iron Doped Titania Flower-Like Nanocrystalline Aggregates: Detection of Brookite and Anatase/Rutile Size–Strain Modeling. J. Appl.Cryst. 2013; 46:1874-1876.

[14] Tompsett G A, Bowmaker G A, Coney R P, Metson J B, Rodgers K A, Seakins J M. The Raman Spectrum of Brookite, TiO_2(pbca, Z=8). J. Raman Spectrosc. 1995; 26:57-62.

[15] Katiyars R S, Dawsons P, Hargreaves M M, Wilkinson G R. Dynamics of the Rutile Structure. III. Lattice Dynamics, Infrared and Raman Spectra of SnO_2. J. Phys. C: Solid State Phys. 1971; 4:2421-2431

[16] Cusco R, Llodo E A, Ibanez J, Artus L, Jimenez J, Wang B, Callahan M J. Temperature Dependence in Raman Scattering in ZnO.J. Phys. Rev. B 2007; 75: 165202-(1-11).

[17] Peercy P S, Morosin B. Pressure and Temperature Dependences of the Raman-active Phonons in SnO_2. J. Phys. R. B 1973; 7:2779-2786.

[18] Tauc J, Grigorovici R, Vancu A. Optical Properties and Electronic Structure of Amorphous Germanium. Pysica.StatusSolidi(b) 1966; 15:627-637.

[19]Pankove J I. Optical Processes in Semiconductors, New York, Dover Publication, 1971, p.22 (Chapter 2).

[20] Ghosh R, Basak D, Fujihara S. Effect of Substrate-induced Strain on the Structural, Electrical, and Optical Properties of Polycrystalline ZnO Thin Films. J. Appli. Phys. 2004; 96:2689-2692.

[21] Srikant V, Clarke D R. Optical Obsorption Edge of ZnO Thin Films: Effect of Substrate. J. Appli. Phys. 1997; 81:6357-6364.